environments

MDPI

Article

Dynamic Noise Mapping in the Suburban Area of Rome (Italy)

Roberto Benocci [1,*], Patrizia Bellucci [2], Laura Peruzzi [2], Alessandro Bisceglie [1], Fabio Angelini [1], Chiara Confalonieri [1] and Giovanni Zambon [1]

[1] Department of Earth and Environmental Sciences (DISAT), University of Milano-Bicocca, Piazza della Scienza 1, 20126 Milano, Italy
[2] ANAS S.p.A., Via della Stazione di Cesano 311, 00123 Cesano di Roma, Italy
* Correspondence: roberto.benocci@unimib.it

Received: 5 May 2019; Accepted: 2 July 2019; Published: 4 July 2019

Abstract: A "real-time" noise mapping project, named DYNAMAP, has been developed in the framework of a Life+ 2013 program and cofunded by the European Commission. The project aims at giving a real picture of the noise generated by vehicular traffic. To this purpose, a dedicated platform has been developed to elaborate the information from distributed noise monitoring stations. The methodology has been implemented along the ring road encircling the city of Rome (Italy). A detailed description of the system is given together with a report on the testing campaign that allowed evaluation of the accuracy and reliability of the system. From the monitoring campaign satisfactory results have been achieved, showing an average overall prediction error of ~1.5 dB.

Keywords: noise mapping; noise mitigation; DYNAMAP project

1. Introduction

Noise pollution was revealed to be one of Europe's major concerns, as firstly reported in the Environmental Noise Directive (END) of 2002 [1] and, later, in its more recent revision [2]. Both versions recognize the importance of monitoring and mapping the sound pressure levels of transport infrastructures to evaluate and control noise exposure. Particularly, road traffic noise is the foremost health problem in Europe [3], with more than 100 million of people exposed to Lden level higher than 55 dB(A). To noise exposure can be attributed a series of health problems, such as sleep disturbance [4,5], annoyance [6], cardiovascular illness [7,8], learning impairment [9,10], and hypertension ischemic heart disease [11]. In order to assess the impact of the main transport infrastructures and to solicit appropriate mitigation actions, the END prompts for a periodic update of noise maps as a result of possible changes in traffic, mobility, and urban scenarios. However, noise mapping activities are quite expensive and time consuming, requiring substantial financial efforts to fulfill END obligations. Thus, cheaper solutions to decrease noise mapping costs are strongly recommended and pursued by local and national road authorities.

Costs and time consumption can be likely reduced by automating the noise mapping process in terms of single input data to feed the noise model, as well as in terms of noise mapping system as a whole.

A first attempt to automate the process was made in 2003 [12], when the Municipality of Madrid, together with Brüel&Kjær, decided to develop a new concept of data post-processing, based on dynamic noise maps or SADMAM (Sistema Actualización Dinámica Mapa Acústico Madrid). Mobile monitoring devices equipped with GIS systems were used to measure sound pressure levels at strategic places. To that end, the municipality of Madrid invested in a system including Lima Noise Calculation Software, Noise Monitoring Software, and several Noise Monitoring Terminals. This approach was

intended to help the city to efficiently validate and improve the quality of strategic noise maps, as well as to support the preparation of the action plan according to END requirements, avoiding unnecessary actions based on poor accurate results.

However, some critical issues emerged from this experience: First of all the need of mobile monitoring devices to sample sound pressure levels. This solution was quite expensive and prevented the automatic updating of noise maps. Secondly, no algorithm for eliminating spurious events, i.e., noise events unrelated to the road traffic, was used to guarantee data reliability and provide accurate maps. In addition, very complicated and time consuming algorithm and software were used to update noise maps, thus drastically reducing the possibility of enhancing the system to real time noise maps.

Another experience came from Paris the same year, with the publication of a dynamic noise map fed by road traffic noise measurements on a daily basis. In this case class I sound level meters and traditional acoustic simulation software were used. This kind of application, although extremely appealing from a technical perspective, was very expensive, due to the high cost of the devices used to measure the noise levels, thus temporarily aborting the attempt of automating the noise mapping process.

In 2008 the Polish Gdansk University of Technology tempted a new approach based on ray tracing techniques running on cluster-type supercomputers. Very accurate, but quite expensive maps were produced, leaving the problem of costs and processing time unresolved [13].

In De Coensel et al. [14], an approach for calculating dynamic noise maps on the basis of fixed as well as mobile sound measurements has been proposed. It extends the temporal and spatial resolution of the traditional noise map that is based on long-term equivalent levels, and is therefore well suited for the prediction of indicators that are more closely related to the perception of the acoustic quality of the urban environment.

Nevertheless, in 2011 another project, named SENSEable PISA (Italy) [15], opened up new perspectives, by developing and implementing low cost monitoring devices. In this project large volumes of environmental data were gathered to extrapolate information on public health, urban mobility, air pollution, etc., using appropriate mathematical tools (data mining).

Taking inspiration from the latter experience, in 2014 a LIFE project called DYNAMAP [16] was cofunded by the European Commission in the framework of the Life+ 2013 program, with the aim of facilitating and accelerating the noise mapping process. To do so, an automatic monitoring system, composed of low-cost sensors and of a powerful software platform was developed and implemented in two pilot areas located in the agglomeration of Milan (Italy) and along the Motorway A90 (Rome-Italy). Noise maps in this case are updated using a smart algorithm based on precalculated noise maps prepared for different traffic and weather conditions [17,18].

The DYNAMAP project is now performing the final step, where the accuracy, reliability and sustainability of the system are being assessed [19–21].

In this paper a detailed description of the system installed in the pilot area of Rome is given, together with a report on the testing campaign undertaken and of the main results achieved.

2. Methods—The DYNAMAP System

DYNAMAP is a dynamic noise mapping system that performs the update of noise maps by means of a combination of dedicated monitoring sensors, software tools and a GIS platform. The system relies on the update of precalculated basic noise maps. This process, denoted as noise map scaling, is accomplished for different operating conditions (sources, traffic and weather conditions), by detecting noise and meteorological data from low-cost monitoring stations and weather sensors distributed along the road. The scaled basic noise maps, one for each elementary noise source present in the mapping area, are summed together to obtain the complete noise map. This process is expected to considerably reduce the use of simulation tools, thus decreasing calculation times and costs. In addition, the development of low-cost noise monitoring stations and the use of a GIS platform for

implementing the maps scaling and their energetic sum, further reduces operational costs. These considerations make the DYNAMAP system a versatile and unique noise mapping tool that can be easily interfaced with the new European model CNOSSOS [22], expected to be operative within 2022. DYNAMAP is also equipped with an anomalous noise events detection algorithm that detects and removes all noise contributions that cannot be attributed to the road traffic.

2.1. Implementation of the DYNAMAP System in the Pilot Area of Rome

The DYNAMAP system has been built in the ninth district of the city of Milan and in Rome, along the ring road encircling the town. Given the different environmental features of the two pilot areas, a diverse approach was used to size and set up the DYNAMAP system. In the pilot area of Milan a statistical approach was employed [23–25], while in the pilot area of Rome a deterministic method was applied. In the following paragraphs, a detailed description of the design and configuration of the system installed in the pilot area of Rome is reported, starting from the selection of the test sites, up to the preparation and update of the basic noise maps.

2.2. Pilot Area Selection

The pilot area of Rome is located along a major road, i.e., the ring road (Motorway A90) surrounding the city, known as Grande Raccordo Anulare (GRA).

The Motorway A90, as many other major roads, crosses suburban complex scenarios that include connections to a variety of transport infrastructures. In these contexts, the noise level at receivers is given by the contributions from all noise sources present in the mapping area. Therefore, the acoustic characterization of the Motorway A90, as well as its noise impact assessment, should avoid exogenous contributions, as required by the END, and simply provide a measure of the sound power level due to the main road axis and its several junctions. Consequently, appropriate positions for the sensors should be identified in order to make the contributions from the other noise sources negligible.

The pilot area of Rome is composed of many test sites that were selected on the basis of technical and environmental characteristics of the road. Sixty-seven elementary areas, centered on the road axis and 250 m wide each side, were considered. Road stretches impacting suburban areas were identified, based on the results achieved from the first and second strategic noise mapping cycles. Satellite images and photographs available on internet (Google Maps) were also used to check the presence of additional noise sources and integrate the morphological description of the sites.

From these data four priority lists, corresponding to as many site types representative of the main suburban scenarios, were identified as follows.

A. Single road (A90 Motorway).
B. Additional crossing or parallel roads.
C. Railway lines running parallel or crossing the A90 motorway.
D. Complex scenario including multiple connections.

Out of 67 sites reported in the priority lists, only the top seventeen have been selected to host the DYNAMAP sensors (Figure 1). In the selection process, particular emphasis was given to those areas where high noise levels were highlighted and where monitoring activities would help to maintain control of the acoustical scenarios.

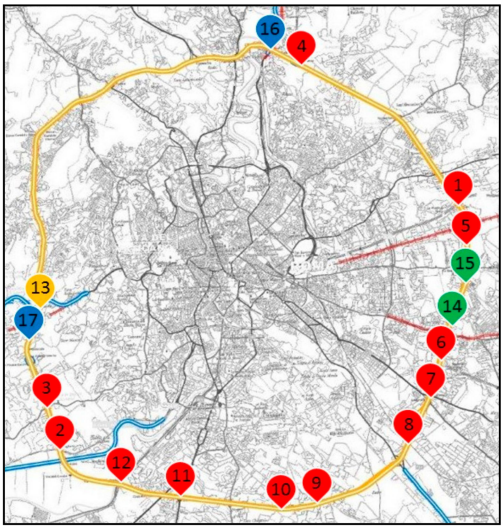

Legend

- Ranking list A—Single road critical areas (from n. 1 to 12)
- Ranking list B—Critical areas with additional crossing or parallel roads (n. 13)
- Ranking list C—Critical areas with railways crossing or running parallel the A90 motorway (nn. 14-15)
- Ranking list D—Complex critical areas with multiple connections (nn. 16-17)

Figure 1. Rome pilot area. In red are reported the locations related to the ranking list A; in yellow the hot spots related to the ranking list B; in green the areas related to the ranking list C; and in blue those related to the ranking list D.

2.3. *Design and Configuration of the System*

In suburban areas, the presence of multiple noise sources and the influence of meteorological conditions on sound propagation can strongly affect the overall noise level at receivers.

The amount of noise sources determines the number of sensors necessary to monitor the mapping area and the quantity of the corresponding basic noise maps required to provide the overall noise map. Therefore, a preliminary study on the noise sources present in the mapping area must be undertaken in order to reduce the number of road stretches to be monitored.

The influence of meteorological conditions on sound propagation is relevant only in suburban areas, where usually receivers are located at a greater distance from the road (≥80 m). In this case, different basic noise maps must be prepared for each propagation condition. This requires the monitoring of meteorological conditions and the conversion of this information in classes of acoustic propagation (favorable, unfavorable, or homogeneous).

2.3.1. Clustering Procedure to Reduce the Number of Elementary Noise Sources

The DYNAMAP system configuration is based on the concept of "elementary noise source". An elementary noise source is a road arc with homogeneous traffic conditions (Figure 2). Since for each elementary noise source a monitoring device should be installed, the size of the DYNAMAP system mainly depends on the number of elementary noise sources present in the mapping area.

Figure 2. An example of elementary noise sources identification.

In order to reduce the number of monitoring devices to be installed and of the basic noise maps to be prepared a clustering procedure was adopted with the aim to find appropriate correlation factors to link different road stretches. To that end, an extensive monitoring campaign was carried out based on an experimental technique aimed at reducing the measurement points as much as possible. This technique took inspiration from Kirchhoff law and makes use of a simplified scheme, where three monitoring points are identified for each carriageway. Two of them are monitored with a sound level meter placed on the main road axis and the other one with a traffic counter placed on a secondary arc, in order to avoid the noise contribution from the main road. Measured data are then easily translated into sound power levels and used to feed the noise model. The sound power levels related to the remaining arcs are then assessed by means of simple mathematical equations.

From the measured data, opportunely converted into sound power levels, the hourly correlation coefficient can be calculated between the different arcs according to the following formula.

$$\Delta(h)_{i,j} = L_w(main\ axis)_{i,j} - L_w(junction)_{i,j} \quad (1)$$

where

- $\Delta(h)_{i,j}$ is the hourly coefficient related to the *i-th* junction and the *j-th* hour;
- $Lw(main\ axis)_{i,j}$ is the hourly sound power level related to the *i-th* measurement position on the main road axis associated with the *i-th* junction and the *j-th* hour; and
- $Lw(junction)_{i,j}$ is the hourly sound power level related to the *i-th* junction and the *j-th* hour.

Then, a detailed analysis was carried out to check the data variability and to identify the most appropriate aggregation class. An iterative approach was used starting from a preliminary study on the measured hourly data. Due to their similar trend during all over the day, it was possible to reduce the hourly coefficients up to daily and at most weekly data [18].

At the end of the process, the whole set of elementary noise sources was clustered into two groups. Each group is characterized by different correlation factors that can be used to monitor and map together different road arcs. The first cluster includes road arcs with regular traffic all over the whole week, including weekends, where a unique correlation coefficient can be used; the second cluster encloses road arcs with different traffic flows in working and weekend days, that need to be characterized by diverse correlation coefficients. Finally, a total of 19 elementary noise sources was identified, of which nine main arcs, with related junctions, ascribed to Cluster 2, and 10 main arcs, with related junctions, ascribed to Cluster 1.

2.3.2. Evaluation of the Influence of Weather Conditions on Sound Propagation

In suburban areas weather conditions can alter noise levels at receivers located at a greater distance from the road (≥80 m), due to favorable, unfavorable, and homogeneous sound propagation conditions. This means that different basic noise maps must be prepared as a function of meteorological conditions and that weather conditions must be monitored in order to identify the most suitable basic noise map to be updated.

In order to reduce the number of basic noise maps to be prepared, and consequently the cost of the system, an in depth study was undertaken to investigate the acoustic model sensitivity to spatial weather variations [18]. The results achieved show that the model is insensitive to small weather variations and that the information gathered by one meteorological station is sufficient to classify sound propagation conditions with an accuracy of 85%.

The same analysis was then carried out to see how sensitive the model to wind direction is [18]. Results showed that the uncertainty associated with wind direction can be reduced by increasing the wind sectors width from 20° to 90°. This solution allows to considerably reduce the number of basic noise maps to be prepared to only four wind sectors (North, East, South, and West) (Figure 3).

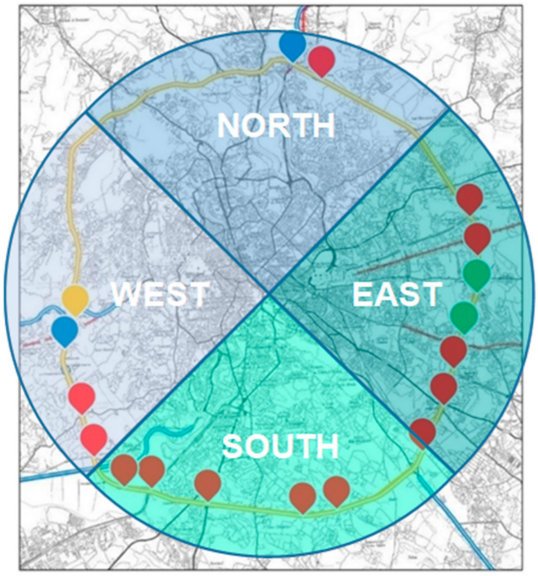

Figure 3. The four wind sectors of the pilot area of Rome.

In the end, only six basic noise maps were found to be necessary to cover the whole set of possible different sound propagation conditions:

- a map for totally favorable conditions;
- a map for totally homogeneous conditions; and
- four maps for favorable conditions in the main wind sectors.

2.4. Basic Noise Maps Preparation and Update

A basic noise map is a static map that reports the contribution of the elementary noise sources present in the mapping area.

The basic noise maps have been prepared using the standard NMPB model (NMPB Route 96/XPS 31-133) implemented in commercial calculation software.

The number of calculations needed to prepare the basic noise maps depends on the method used to accomplish the maps. For the pilot area of Rome the grid noise map method was applied and for each elementary noise source separate simulations were made in order to achieve its contribution to the overall noise level.

In the pilot area of Rome 19 elementary noise sources have been identified: nine main arcs, with related junctions ascribed to Cluster 2, and 10 main arcs, with related junctions ascribed to Cluster 1. This involved the preparation of $(10 \times 1) + (9 \times 2) = 28$ basic noise maps. Furthermore, for each elementary noise source, six meteorological conditions were taken into account, leading to a total number of 168 calculations.

To summarize, 12 basic noise maps were prepared for each elementary noise source, as a function of meteorological (6) and traffic conditions during the week (2).

The preparation of the basic noise maps entailed the following steps.

- To split the road network in stretches corresponding to the elementary noise sources (Figure 4);
- To generate a unique grid for the whole pilot area, to avoid mismatching when summing up the different maps, and to prepare a unique calculation area corresponding to a buffer of 250 m each side around the ring road (Figure 5); and
- To turn on one elementary noise source at a time and calculate the whole set of basic noise maps in the whole calculation area (Figure 6).

Figure 4. Basic noise maps preparation: split the road network in arcs corresponding to the elementary noise sources.

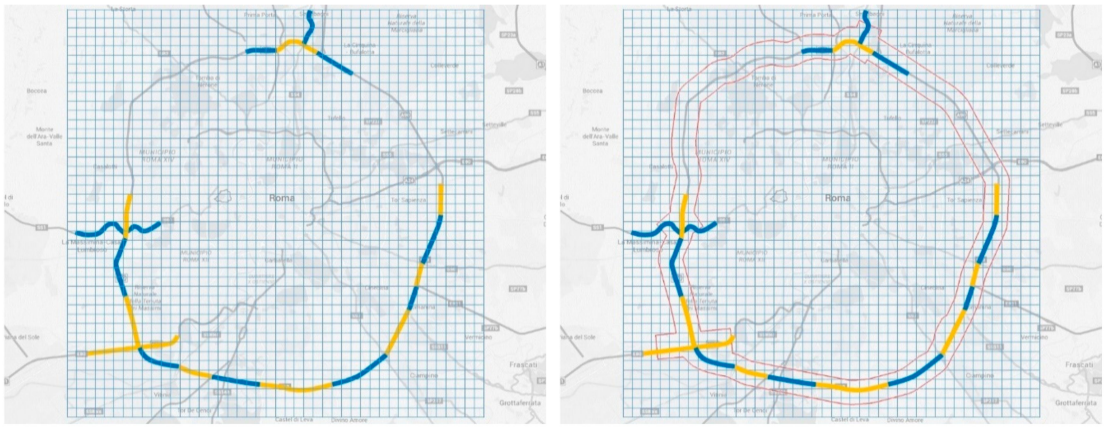

(**a**) (**b**)

Figure 5. Basic noise maps preparation: generate a unique grid for the whole pilot area (**a**) and prepare a unique calculation area (**b**).

Figure 6. Basic noise maps preparation: turn on one elementary noise source at a time and calculate the basic noise maps in the whole calculation area.

The complete map was achieved by summing up the whole set of noise map related to each elementary noise source, even though in general the overall level is influenced by two or three sources at the most.

As shown in Table 1, basic noise maps are summarized in arrays that report on each row the contribution of the elementary noise sources to one point of the grid. In detail, the first column of the

array shows the identification code of the grid point (ID), followed by its coordinates and the noise level contribution of each elementary noise source to that point.

The last column reports the overall noise level given by the sum of the contributions related to that point, according to the following Formula.

$$LeqR_j = 10 \log \sum_{i=1}^{N} 10^{0.1 Leq_{j,i}}. \quad (2)$$

where

- $LeqR_j$ is the final equivalent noise level associated with the *j-th* grid point;
- $Leq_{j,i}$ is the equivalent noise level related to the *j-th* grid point and the *i-th* elementary noise source; and
- N is the number of elementary noise sources.

Table 1. Basic noise map array.

ID	LAT	LONG	NS1 dB(A)	NS2 dB(A)	NS3 dB(A)	…	NSN dB(A)	Leq $_T$ dB(A)
0001	X0001	Y0001	L_{11}	L_{12}	L_{13}	…	L_{1N}	Leq_{R1}
0002	X0002	Y0002	L_{21}	L_{22}	L_{23}	…	L_{2N}	Leq_{R2}
…	…	…	…	…	…	…	…	…
…	…	…	…	…	…	…	…	…
…	…	…	…	…	…	…	…	…
…	…	…	…	…	…	…	…	…
9999	X_{9999}	Y_{9999}	L_{99991}	L_{9992}	L_{99993}	…	L_{9999N}	Leq_{R9999}

The table shows the identification code of the grid point (ID), followed by its coordinates (latitude LAT and longitude LONG) and the noise level contribution of each elementary noise source to that point (NS, from NS1 to NSN). The last column shows the overall noise level given by the sum of the contributions related to that point (Leq $_T$).

Since each column refers to a single elementary noise source, the update of the map is achieved by scaling the corresponding data according to the noise level detected by the monitoring stations. The amount to be scaled is given by the difference between the measured values and the calculated values at reference points corresponding to the positions of the monitoring stations. An additional array has been prepared to report the calculated noise levels at the reference points.

In Figure 7 an example of basic noise map is reported. For an arbitrary grid point of the base map, identified by its ID number (ID = 312535 in the example), the predicted value of LeqT is calculated as the sum of the contributions of the most significant sensors (S12, S13, and S14), and updated every 30s (in the example the values LeqT are shown at the arbitrary T_0 = 0 s and at T_1 = 30 s). These contributions are obtained by comparing the level values measured by each sensor with the ones at the reference point; this allows the calculation of Delta used for updating the acoustic map.

Time T_0 = 0 s

Elementary noise source n.				S1	S2	S3	S4	S5	S6	S7	S8	S9	S10	S11	S12	S13	S14	S15	S16	S17	S18	S19	
Value at reference point				79.7	78.8	75.5	75	78.3	79.4	79	80.8	76.3	80.8	77.3	78.4	79.3	74.6	78.8	70.8	70	76.2	78.6	
Measured value by sensor				79.2	78.8	76	75.6	78.2	78.8	78.6	80.7	77	81	77	79	80	75.1	78.3	71.1	71.2	75.9	78.1	
Delta				-0.5	0	0.5	0.6	-0.1	-0.6	-0.4	-0.1	0.7	0.2	-0.3	0.6	0.7	0.5	-0.5	0.3	1.2	-0.3	-0.5	
ID	X	Y	Z	S 1	S 2	S 3	S 4	S 5	S 6	S 7	S 8	S 9	S 10	S 11	S 12	S 13	S 14	S 15	S 16	S 17	S 18	S 19	LeqT
312535	42	13	60	0	0	0	0	0	0	0	0	0	0	0	68.5	20.7	31.6	0	0	0	0	0	69.1

Time T_1= 30 s

Elementary noise source n.				S1	S2	S3	S4	S5	S6	S7	S8	S9	S10	S11	S12	S13	S14	S15	S16	S17	S18	S19	
Value at reference point				79.7	78.8	75.5	75	78.3	79.4	79	80.8	76.3	80.8	77.3	78.4	79.3	74.6	78.8	70.8	70	76.2	78.6	
Measured value by sensor				79	78.5	75.9	75.3	78	79.5	78.3	81	76.8	81.2	77.9	79.2	80.4	75.3	78.5	70.8	70.2	76	78.4	
Delta				-0.7	-0.3	0.4	0.3	-0.3	0.1	-0.7	0.2	0.5	0.4	0.6	0.8	1.1	0.7	-0.3	0	0.2	-0.2	-0.2	
ID	X	Y	Z	S 1	S 2	S 3	S 4	S 5	S 6	S 7	S 8	S 9	S 10	S 11	S 12	S 13	S 14	S 15	S 16	S 17	S 18	S 19	LeqT
312535	42	13	60	0	0	0	0	0	0	0	0	0	0	0	70.3	21.9	32.9	0	0	0	0	0	69.3

Figure 7. Example of a map update related to point grid ID = 312535 at time T_0 = 0 s and after 30 s (T_1 = 30 s).

The same kind of approach was used for the calculation of the maximum noise level at the most exposed façade. In this case the array reports the ID and position of the receiver, its height or floor, and the contribution of each elementary noise source, together with the overall noise level. The update of the noise level at receivers is achieved using the same procedure described for the noise maps. Each column, corresponding to the contribution of the different noise sources, is updated as a function of the noise level detected by the monitoring stations.

When updating the map, i.e., the noise levels at grid points, the most suitable basic noise map must be selected. The selection of the appropriate basic noise map (array) as a function of meteorological conditions is accomplished by converting measured meteorological conditions into sound propagation conditions. To do so, smart algorithms have been developed and implemented in a WEB GIS platform, whose main role is to manage and update the noise maps.

In the pilot area of Rome noise maps are updated with a time frequency of 30 s from 6:00 a.m. to 10:00 p.m. At night, when traffic flow is lighter and less continuous, noise maps are updated every 5 min.

3. Measuring Campaign

In order to verify the accuracy and reliability of the DYNAMAP system, two measuring campaigns (winter 2017 and summer 2018) have been performed, which allowed to compare the values achieved by the system and the field measurements distributed around the GRA area.

To that end, the DYNAMAP system was equipped with a dedicated algorithm embedded in the noise sensors for the detection of anomalous noise events (ANEs), i.e., noise events unrelated to road traffic noise [26–28]. Therefore, also the recorded data required to be manually cleaned up using the procedure described in Alsina-Pagés et al. [29].

Measurements were accomplished using a free-field microphone positioned at 4m height and had a duration of 1 h. They were performed in different environmental conditions and configurations, i.e., single and coupled measurements (in-line) at two different distances from the source.

All sites have been chosen according to morphological and infrastructural characteristics of the area. This choice allowed testing the system in highly complex contexts with the presence of barriers, embankments, secondary roads, etc.

3.1. Winter and Summer Campaign

Two measuring campaigns have been carried out: a preliminary winter campaign (2017) followed by a summer session in 2018. The first session allowed to highlight some criticalities connected to the

system settings and simulation model, whereas the latter confirmed the upgraded improvements. In Figure 8, the positions of the measuring sites and of the DYNAMAP sensors are illustrated; in Table 2, for each measuring site, the geographical coordinates and the corresponding distance from the traffic noise source are reported.

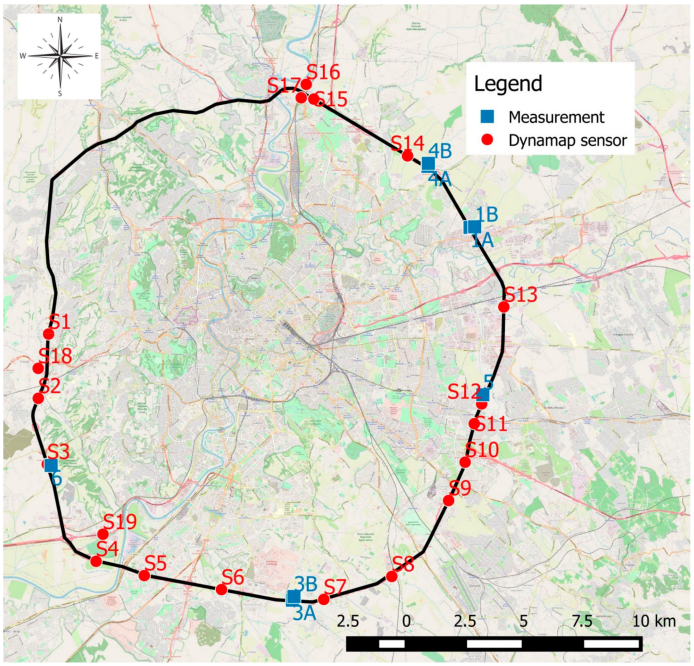

Figure 8. DYNAMAP sensors position (red spots) along the A90 motorway and measuring sites (blue squares) during the summer measuring campaign.

Table 2. Measuring sites, geographical coordinates, and distance from the A90 Motorway axis.

Site	Latitude	Longitude	Distance from A90 [m]
1A	41°56′15.4″ N	12°35′53.6″ E	15
1B	41°56′16.2″ N	12°36′02.2″ E	195
3A	41°47′41.1″ N	12°30′25.2″ E	25
3B	41°47′46.3″ N	12°30′28.0″ E	190
4A	41°57′39.6″ N	12°34′35.8″ E	55
4B	41°57′43.8″ N	12°34′36.6″ E	180
5	41°52′24.6″ N	12°36′17.2″ E	90
6	41°50′47.1″ N	12°22′59.0″ E	100

3.2. *Description of the Measurement Sites*

In this section, we describe the characteristics of each site in order to better understand and interpret the measurement results.

3.2.1. Site 1A-1B

Site 1 is characterized by two in-line measurements. In particular, Site 1A is located 15 m away from the main noise source with in between a secondary less congested road. Site 1B is 195 m away from the GRA with in between an uncultivated lawn and the secondary road. The terrain vertical section corresponding to sites 1A and 1B is illustrated in Figure 9. The employed basic noise map is WD-WEST corresponding to working day and favorable conditions in the western wind sector.

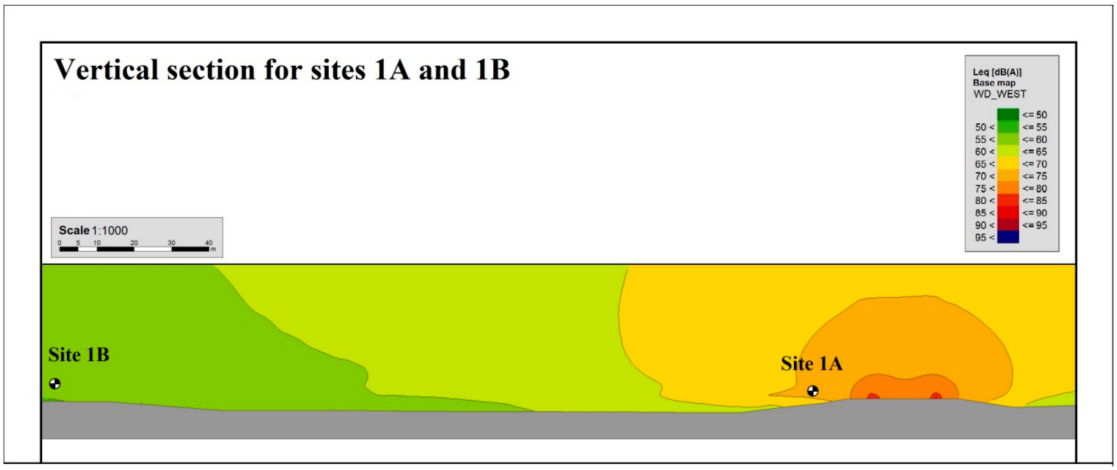

Figure 9. Terrain vertical section corresponding to sites 1A and 1B. Soil characteristics: uncultivated lawn, plain. Equivalent level intervals are displayed with different colors. Levels calculated according to the Basic Noise Map WD-WEST.

3.2.2. Sites 3A-3B

Site 3 is characterized by two in-line measurements. Both sites are in a cultivated terrain; Site 3A is 25 m away from the GRA with in between a vegetation barrier. Site 3B is 190 m away from GRA at greater height with respect to the motorway altitude and with a secondary road in the vicinity. The terrain vertical section corresponding to sites 3A and 3B is illustrated in Figure 10. The employed basic noise map is WD-HOM, corresponding to working day and totally homogeneous conditions.

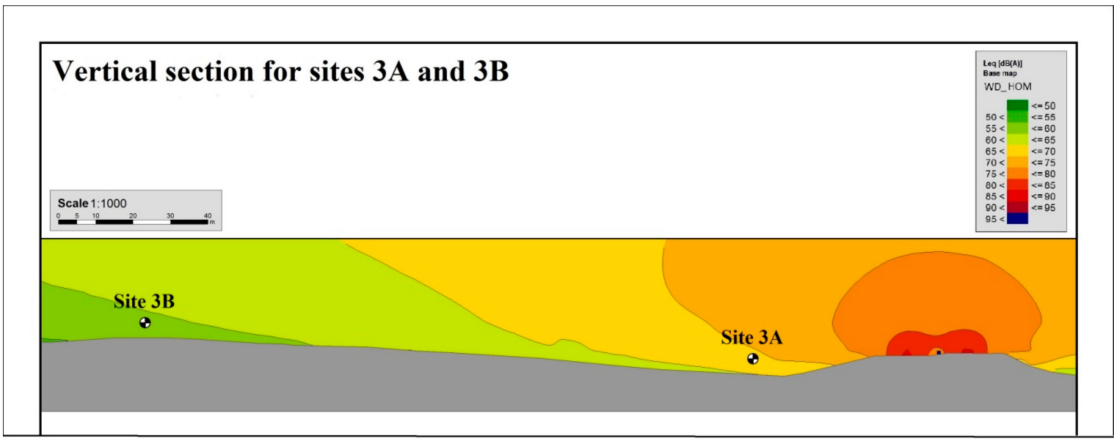

Figure 10. Terrain vertical section corresponding to sites 3A and 3B. Soil characteristics: cultivated field, presence of vegetation barrier, Site 3B in elevated position. Equivalent level intervals are displayed with different colors. Levels calculated according to the Basic Noise Map WD_HOM.

3.2.3. Sites 4A–4B

Site 4 is characterized by 2 in-line measurements. Both sites are in an uncultivated terrain; Site 4A is at 55 m from the GRA with in between a light depression. Site 4B is at ~180 m away from the GRA in the proximity of a bush and with a secondary road in the vicinity. The terrain vertical section corresponding to sites 4A and 4B is illustrated in Figure 11. The employed basic noise map is WD-HOM, corresponding to working day and totally homogeneous conditions.

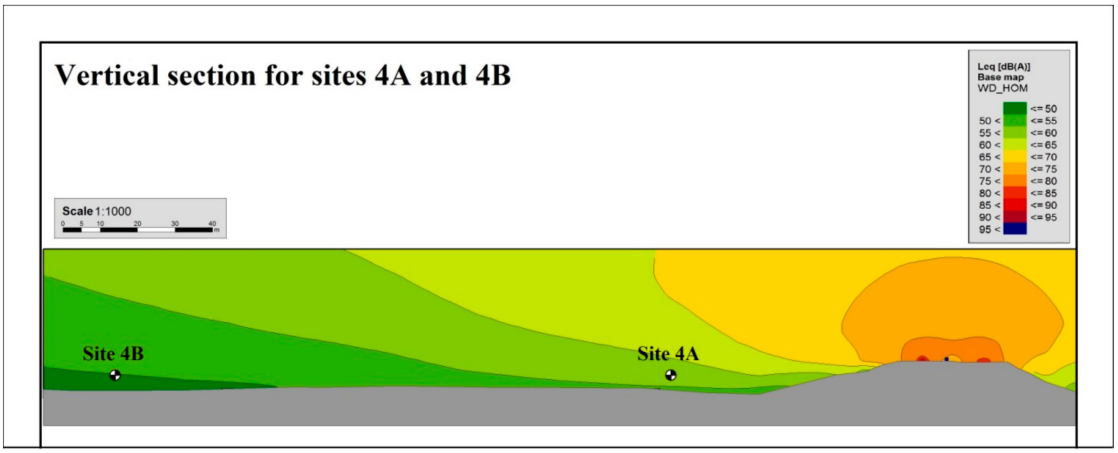

Figure 11. Terrain vertical section corresponding to sites 4A and 4B. Soil characteristics: uncultivated field, site 4A in depressed position, site 4B close to a bush. Equivalent level intervals are displayed with different colors. Levels calculated according to the Basic Noise Map WD_HOM.

3.2.4. Site 5

Site 5 is characterized by a single measurement and located in a playground in the vicinity of a residential area and at distance from GRA of about 90 m. A noise barrier is installed along the GRA in between the source and the measurement site. In this case, the time duration of the measurement was 45 min. The terrain vertical section corresponding to Site 5 is illustrated in Figure 12. The employed basic noise map is WD-HOM, corresponding to working day and totally homogeneous conditions.

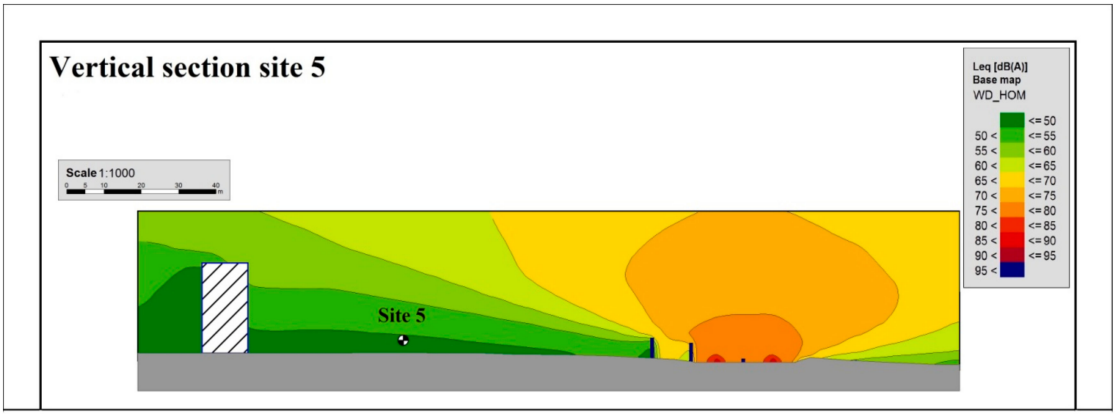

Figure 12. Terrain vertical section corresponding to Site 5. Soil characteristics: playground, vicinity to residential area. Equivalent level intervals are displayed with different colors. Levels calculated according to the Basic Noise Map WD_HOM.

3.2.5. Site 6

Site 6 is characterized by a single measurement. The measurement location is an uncultivated field, above-ground with respect to GRA. Its distance is 100m from the main source of traffic noise. The terrain vertical section corresponding to Site 6 is illustrated in Figure 13. The employed basic noise map is WD-HOM, corresponding to working day and totally homogeneous conditions.

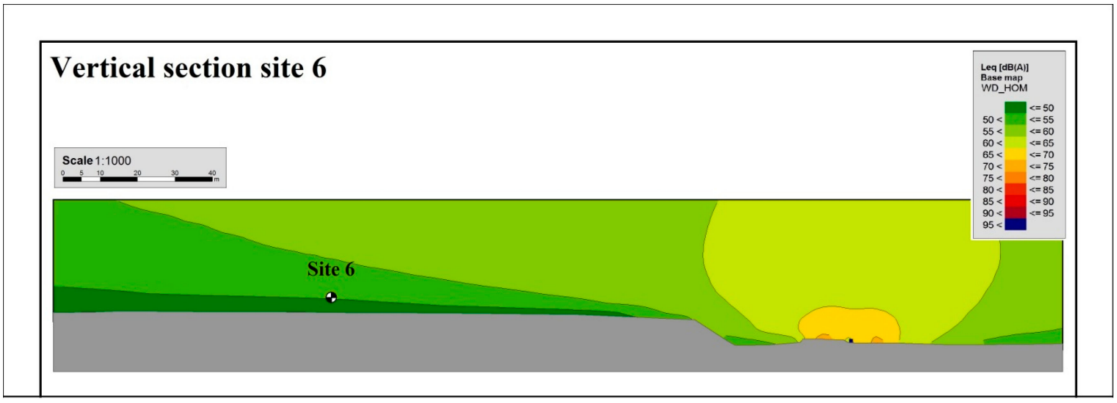

Figure 13. Terrain vertical section corresponding to Site 6. Soil characteristics: uncultivated field and above-ground with respect to the GRA. Equivalent level intervals are displayed with different colors. Levels calculated according to the Basic Noise Map WD_HOM.

3.3. DYNAMAP System Accuracy

The analysis that followed the preliminary winter monitoring session showed some criticalities connected to an incorrect assignment of the ground factor to the noise propagation model. Its implementation allowed a more correct evaluation of the base noise maps described above.

In the following figures, we report the comparison between DYNAMAP predictions and measurements in two test sites during the final summer monitoring campaign. In Figures 14 and 15, the A-weighted 30 s equivalent level for sites 3A and 6 is illustrated, with the corresponding root mean square deviation, $<\sigma_{rms}>$, calculated over the measurement duration (1 h), is reported. $<\sigma_{rms}>$ is expressed by

$$< \sigma_{rms} > = \sqrt{\frac{1}{N}\sum_{i=1}^{N}\left(Leq_{D_i} - Leq_{M_i}\right)^2} \quad (3)$$

where Leq_D, Leq_M and N are the predicted and measured equivalent levels calculated on a time basis of 30 s and N the number of points in 1 h (N = 120), respectively.

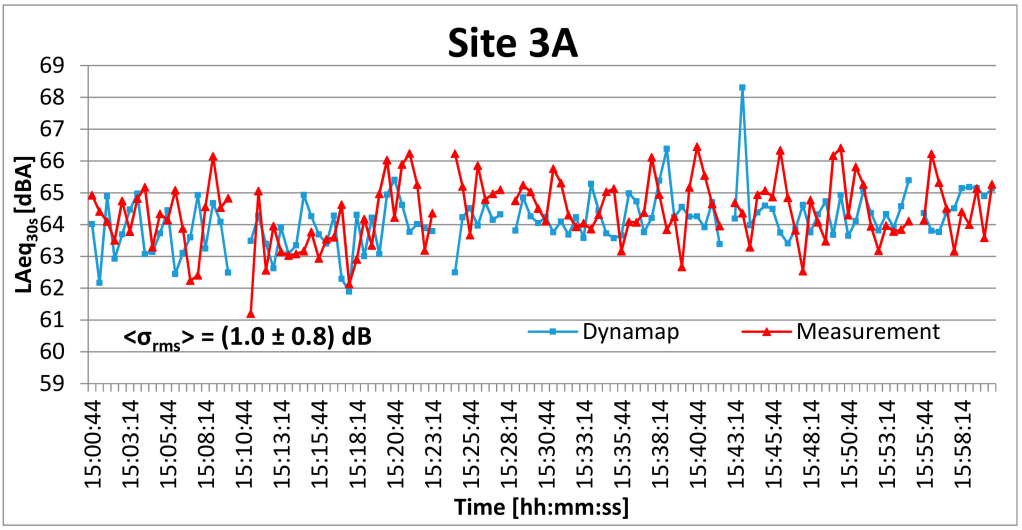

Figure 14. Comparison between DYNAMAP prediction (blue line) and measurement (red line) for Site 3A (summer 2018 campaign). On the ordinate, the A-weighted 30 s equivalent level is shown. All anomalous events have been removed from both time series.

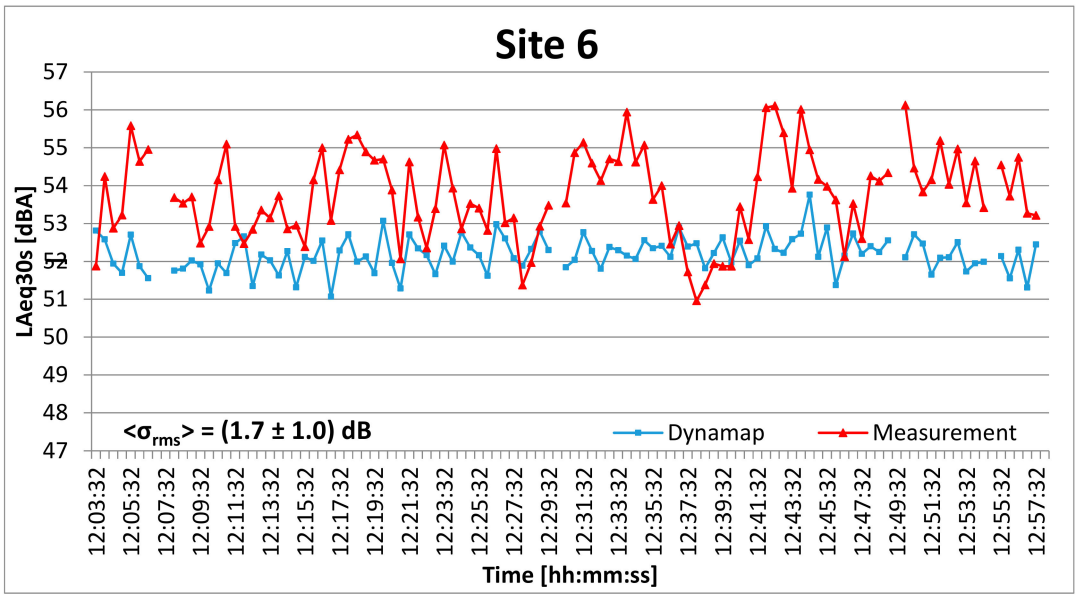

Figure 15. Comparison between DYNAMAP prediction (blue line) and measurement (red line) for Site 6 (summer 2018 campaign). On the ordinate, the A-weighted 30 s equivalent level is shown. All anomalous events have been removed from both time series.

From both time series, all anomalous events have been removed (see interruption in Figures 14 and 15).

In Table 3, the summary of the results obtained for all monitored sites is shown.

Table 3. Summary of results: comparison between DYNAMAP predictions and measurements in all sites.

Site	$<\sigma_{rms}>$ [dB]
1a	1.8 ± 0.7
1b	1.0 ± 0.8
3a	1.0 ± 0.8
3b	1.5 ± 1.2
4a	1.7 ± 1.1
4b	1.8 ± 1.2
5	1.5 ± 0.9
6	1.7 ± 1.0

As we can observe, the prediction deviation is reasonably satisfactory with an overall mean deviation of 1.5 dB. As a general remark, we can observe how the root mean square deviation, $<\sigma_{rms}>$, for Site 1A and 1B decreases at a larger distance, from 15 to 195 meters, in contrast to sites 3 and 4, for whom we observe an increase. This fact can be attributed to different causes: firstly, the elevated position of Site 3B and, secondly, the presence of a secondary road in the vicinity of Site 4B. These characteristics might increase the background contribution, therefore, affecting the measurements.

4. Discussion

The results achieved show a good accuracy of the DYNAMAP system, even though many problems have been experienced in measuring the noise signals, especially at great distance from the road axis, due to the influence of additional locally distributed noise sources (background noise).

Background noise affects the signal dynamics. As it can be seen from Figures 8 and 9, the dynamics of the measured noise levels are ~2 dB higher than the dynamics of the corresponding estimated noise levels. This effect is particularly relevant away from the road, where the background noise tends to overcome the road noise coming from the primary source. In this case, the noise signal is affected by the nearest noise sources.

Figures 8 and 9 also highlight a different temporal behavior of the two signals. This is due not only to the influence of the background noise, but also to the time shift between the noise levels at the measuring point and sensor position. The time shift depends also on the average traffic speed. In free flowing traffic conditions and at normal speed, time shifts give rise to different temporal trends. Instead, at high speed the time correlation between the two signals tends to decrease. Likewise, at low speed, corresponding to congested traffic, the noise source could be considered stationary (linear source) and the temporal shift irrelevant.

The correlation between measured and estimated time series can be improved by increasing the integration time or by reducing the sensors spatial frequency. Further studies are in progress to deepen this effect and to improve the predictive algorithm in order to properly take into account time shift phenomena. More tests will be undertaken to investigate the system response in different environmental scenarios and at different updating frequencies (from 30 s up to 60 min).

Another test was also performed to check the systematic error introduced by the DYNAMAP system. In this test, the estimated levels were translated in order to achieve the same overall equivalent noise level of the measured signal. In this way the estimated signal is treated as the model was perfectly calibrated, so that the results only depend on the accuracy of the system itself. The outcome of this test has shown that the average prediction deviation is ~1 dB. This corresponds to the systematic error introduced by the DYNAMAP system.

5. Conclusions

This paper describes the DYNAMAP system implemented in the pilot area of Rome. The description includes information on the system configuration and on the solutions developed to prepare and update the noise maps in real time. In order to validate the system, two field measuring campaign were arranged: the first one in winter 2017 and the second one in summer 2018. These monitoring campaigns also involved the detection of the noise levels at specific receiver points and the comparison of the results with the corresponding estimated values on the noise map. Their outcomes show an average overall prediction error of ~1.5 dB and a mean systematic error of 1 dB. This highlights a good correlation between measured and estimated noise levels and a satisfactory calibration of the noise model.

This initial testing campaign was limited to the comparison of noise levels measured in arbitrary locations to those predicted by the DYNAMAP system. In these terms, such comparison has been considered satisfactory and promising, as deviations in all tested cases are less than 2 dB. These results, however, are not definitive and deserve a more careful evaluation in order to be confirmed over a long term period, especially in sites where a higher spatial resolution is needed, such as those with nonuniform morphology.

Author Contributions: Data curation, F.A. and C.C.; Formal analysis, L.P., F.A., and C.C.; Investigation, R.B.; Methodology, P.B. and L.P.; Software, L.P.; Supervision, P.B. and G.Z.; Validation, A.B.; Writing—original draft, R.B.; Writing—review & editing, R.B. and P.B.

Acknowledgments: This research has been co-founded by the European Commission under project LIFE13 ENV/IT/001254 DYNAMAP.

Conflicts of Interest: The authors declare no conflict of interest.

References

1. E. Union. Directive 2002/49/EC of the European Parliament and the Council of 25 June 2002 relating to the assessment and management of environmental noise. In *Official Journal of the European Communities L 189/12*; E. Union: Brussels, Belgium, 2002.
2. E. Commission. *Report From The Commission To The European Parliament And The Council On the Implementation of the Environmental Noise Directive in Accordance with Article 11 of Directive 2002/49/EC. COM/2017/0151*; E. Commission: Brussels, Belgium, 2017.
3. Licitra, G.; Ascari, E.; Fredianelli, L. Prioritizing Process in Action Plans: A Review of Approaches. *Curr. Pollut. Rep.* **2017**, *109*, 151–161. [CrossRef]
4. Muzet, A. Environmental noise, sleep and health. *Sleep Med. Rev.* **2007**, *11*, 135–142. [CrossRef] [PubMed]
5. De Kluizenaar, Y.; Janssen, S.A.; Van Lenthe, F.J.; Miedema, H.M.E.; MacKenbach, J.P. Long-term road traffic noise exposure is associated with an increase in morning tiredness. *J. Acoust. Soc. Am.* **2009**, *126*, 626–633. [CrossRef] [PubMed]
6. Miedema, H.M.E.; Oudshoorn, C.G.M. Annoyance from Transportation Noise: Relationships with Exposure Metrics DNL and DENL and Their Confidence Intervals. *Environ. Health Perspect.* **2001**, *109*, 409–416. [CrossRef] [PubMed]
7. Babisch, W.; Beule, B.; Schust, M.; Kersten, N.; Ising, H. Traffic Noise and Risk of Myocardial Infarction. *Epidemiology* **2005**, *16*, 33–40. [CrossRef] [PubMed]
8. Babisch, W.; W, B. Road traffic noise and cardiovascular risk. *Noise Health* **2008**, *10*, 27. [CrossRef] [PubMed]
9. Lercher, P.; Evans, G.W.; Meis, M. Ambient Noise and Cognitive Processes among Primary Schoolchildren. *Environ. Behav.* **2003**, *35*, 725–735. [CrossRef]
10. Chetoni, M.; Ascari, E.; Bianco, F.; Fredianelli, L.; Licitra, G.; Cori, L. Global noise score indicator for classroom evaluation of acoustic performances in LIFE GIOCONDA project. *Noise Mapp.* **2016**, *3*, 157–171. [CrossRef]
11. Van Kempen, E.; Babisch, W. The quantitative relationship between road traffic noise and hypertension: A meta-analysis. *J. Hypertens.* **2012**, *30*, 1075–1086. [CrossRef] [PubMed]
12. Manvell, D.; Ballarin Marcos, L.; Stapelfeldt, H.; Sanz, R. SADMAM–Combining Measurements and Calculations to Map Noise in Madrid. In Proceedings of the Inter-Noise 2004, Prague, Czech Republic, 22–25 August 2004.
13. Kozielecki, P.; Czyzewski, A. An application for vector-based dynamic noise maps generation. In Proceedings of the Joint Baltic-Nordic Acoustics Meeting 2008, Reykjavik, Iceland, 17–19 August 2008.
14. De Coensel, B.; Sun, K.; Wei, W.; Van Renterghem, T.; Sineau, M.; Ribeiro, C.; Can, A.; Aumond, P.; Lavandier, C.; Botteldooren, D. *Dynamic Noise Mapping Based on Fixed and Mobile Sound Measurements*; EURONOISE 2015: Maastricht, France, 2015.
15. Nencini, L.; Ascari, E.; Vinci, B. SENSEable Pisa: A wireless sensor network for real-time noise mapping. In Proceedings of the Euronoise 2012, Prague, Czech Republic, 10–14 June 2012.
16. DYNAMAP. 2014. Available online: http://www.life-DYNAMAP.eu/ (accessed on 22 December 2017).
17. Smiraglia, M.; Benocci, R.; Zambon, G.; Roman, H. Predicting hourly traffic noise from traffic flow rate model: Underlying concepts for the DYNAMAP project. *Noise Mapp.* **2016**, *3*, 130–139.
18. Bellucci, P.; Peruzzi, L.; Zambon, G. LIFE DYNAMAP project: The case study of Rome. *Appl. Acoust.* **2017**, *117*, 193–206. [CrossRef]
19. Benocci, R.; Angelini, F.; Bisceglie, A.; Zambon, G.; Bellucci, P.; Peruzzi, L.; Alsina-Pages, R.M.; Socoró, J.C.; Alías, F.; Orga, F. Initial verification of dynamic acoustic mapping along the motorway surrounding the city of Rome. In Proceedings of the INTER-NOISE and NOISE-CON Congress and Conference Proceedings, Chicago, IL, USA, 26–29 August 2018; The International Institute of Noise Control Engineering (I-INCE): Reston, VA, USA.
20. Benocci, R.; Angelini, F.; Cambiaghi, M.; Bisceglie, A.; Roman, H.E.; Zambon, G.; Alsina-Pagés, R.M.; Socoró, J.C.; Alías, F.; Orga, F. Preliminary results of DYNAMAP noise mapping operations. In Proceedings of the INTER-NOISE and NOISE-CON Congress and Conference Proceedings, Chicago, IL, USA, 26–29 August 2018; The International Institute of Noise Control Engineering (I-INCE): Reston, VA, USA.
21. Benocci, R.; Molteni, A.; Cambiaghi, M.; Angelini, F.; Roman, H.E.; Zambon, G. Traffic Noise Prediction Reliability of DYNAMAP Project. *Appl. Acoust.* (Accepted).

22. Kephalopoulos, S.; Paviotti, M.; Anfosso Lédée, F. *Common Noise Assessment Methods in Europe (CNOSSOS-EU)*; Publications Office of the European Union Report EUR 25379 EN (2002) 1-180; Publications Office of the European Union: Brussels, Belgium, 2002.
23. Zambon, G.; Benocci, R.; Brambilla, G. Cluster categorization of urban roads to optimize their noise Monitoring. *Environ. Monit. Assess.* **2016**, *188*. [CrossRef] [PubMed]
24. Zambon, G.; Benocci, R.; Bisceglie, A. Development of optimized algorithms for the classification of networks of road stretches into homogeneous clusters in urban areas. In Proceedings of the 22nd ICSV, Florence, Italy, 12–16 July 2015.
25. Zambon, G.; Benocci, R.; Brambilla, G. Statistical Road Classification Applied to Stratified Spatial Sampling of Road Traffic Noise in Urban Areas. *Int. J. Environ. Res.* **2016**, *10*, 411–420.
26. Orga, F.; Socoró, J.C.; Alsina-Pagès, R.M.; Zambon, G.; Benocci, R.; Bisceglie, A. Anomalous noise events considerations for the computation of road traffic noise levels: The DYNAMAP' s Milan case study. In Proceedings of the 24th International Congress on Sound and Vibration, London, UK, 23–27 July 2017; pp. 23–27.
27. Socoró, J.C.; Alías, F.; Alsina-Pagés, R.M. An anomalous noise events detector for dynamic road traffic noise mapping in real-life urban and suburban environments. *Sensors* **2017**, *17*, 2323. [CrossRef] [PubMed]
28. Alías, F.; Socoró, J.C. Description of Anomalous Noise Events for Reliable Dynamic Traffic Noise Mapping in Real-Life Urban and Suburban Soundscapes. *Appl. Sci.* **2017**, *7*, 146. [CrossRef]
29. Alsina-Pagés, R.M.; Orga, F.; Alías, F.; Socoró, J.C.; Benocci, R.; Zambon, G. Removing Anomalous Events for Reliable Road Traffic Noise Maps Generation: From Manual to Automatic Approaches. *Appl. Acoust.* **2019**, *151*, 183–192. [CrossRef]